Hydrothermal Synthesis, Structure, and Magnetic Properties of a Layered Organically Templated Uranium Aquofluoride: $[C_5H_{14}N_2][U_2F_{10}(H_2O)]$

Philip M. Almond,[†] Laura Deakin,[‡] Arthur Mar,[‡] and Thomas E. Albrecht-Schmitt*,[†]

Department of Chemistry, Auburn University, Alabama 36849, and Department of Chemistry, University of Alberta, Edmonton, Alberta, Canada T6G 2G2

Received August 11, 2000

Application of a compositional space diagram to the UO_3/HF/homopiperazine ($C_5H_{12}N_2$) system at 180 °C in aqueous media has allowed for the isolation of a unique organically templated U(IV) aquofluoride, $[C_5H_{14}N_2][U_2F_{10}(H_2O)]$ (**AU2-3**) that has been characterized by single-crystal X-ray diffraction, elemental analysis, and magnetic susceptibility measurements. Crystallographic data: **AU2-3**, monoclinic, space group $P2_1/m$, $a = 8.332(4)$ Å, $b = 7.186(3)$ Å, $c = 10.812(9)$ Å, $\beta = 95.07(6)°$, $Z = 2$. The structure of **AU2-3** consists of UF_9 and $UF_8(H_2O)$ tricapped trigonal prisms that share two edges to form $^1_\infty[UF_4F_{4/2}(H_2O)]$ and $^1_\infty[UF_5F_{4/2}]$ chains extending along the *b* direction. These chains are then cross-linked by face-sharing of the tricapped trigonal prisms to yield $^2_\infty[U_2F_{10}(H_2O)]^{2-}$ layers. These layers contain small channels running down the *a* axis that are partially filled with coordinated water molecules. The layers are separated by diprotonated homopiperazine cations that form strong hydrogen-bonding networks. The magnetic susceptibility at temperatures above 150 K reveals a θ value of −15 K and an effective moment of 3.68 μ_B/U(IV), while low-temperature measurements suggest the presence of a nonmagnetic ground state with a linear isothermal magnetization at 2 K and a temperature-independent susceptibility of 0.088 emu/fu (fu ≡ formula unit) below 8 K.

Introduction

The chemistry of uranium in aqueous media, both in the laboratory and under geochemical conditions, is dominated by the formation of U(VI) compounds, the majority of which contain uranyl, UO_2^{2+}, moieties.[1−4] Under reducing conditions, U(IV) becomes the dominant oxidation state[1] as U(V) rapidly disproportionates into U(VI) and U(IV), albeit this process occurs more slowly at low pH.[4−10] However, uranium oxides such as β-U_3O_8 [11] and the mineral wyartite, $CaU(UO_2)_2(CO_3)O_4(OH)(H_2O)_7$, contain U(V) centers.[12] Uranium fluorides and oxyfluorides, which typically contain uranium in the +4 and +6 oxidation states, respectively, have a rich history that was particularly well developed during the mid-20th century.[1,13−15] A considerable portion of this work was borne out of requirements for elemental and isotopic separations as well as the elucidation of the structural chemistry of actinides.[1,13−15]

Recent advances in uranium-based materials have exploited compositional space diagrams[16−18] in organically templated hydrothermal syntheses to systematically study structural relationships and physical properties.[19−23] This approach has led to the isolation of a large series of low-dimensional uranium fluorides,[19−25] oxyfluorides,[20,21,23] molybdates,[26] and phosphates.[27] These studies reveal that aliphatic amines, such as piperazine and homopiperazine, are quite reducing under hydrothermal conditions, resulting in the isolation of both U(IV)

† Auburn University.
‡ University of Alberta.

(1) Carnall, W. T.; Crosswhite, H. M. In *The Chemistry of the Actinide Elements*; Katz, J. J., Seaborg, G. T., Morss, J. R., Eds.; Chapman and Hall: London, 1986.
(2) Burns, P. C.; Miller, M. L.; Ewing, R. C. *Can. Mineral.* **1996**, *34*, 845.
(3) Burns, P. C.; Ewing, R. C.; Hawthorne, F. C. *Can. Mineral.* **1997**, *35*, 1551.
(4) Kraus, K. A.; Nelson, F.; Johnson, G. L. *J. Am. Chem. Soc.* **1949**, *71*, 2510.
(5) Kraus, K. A.; Nelson, F.; Johnson, G. L. *J. Am. Chem. Soc.* **1949**, *71*, 2517.
(6) Coleman, J. S.; Penneman, R. A.; Keenan, T. K.; LaMar, L. E.; Armstrong, D. E.; Asprey, L. B. *J. Inorg. Nucl. Chem.* **1956**, *3*, 327.
(7) Newton, T. W.; Baker, F. B. *Inorg. Chem.* **1965**, *4*, 1166.
(8) Selbin, J.; Ortega, J. D. *Chem. Rev.* **1969**, *69*, 657.
(9) Kern, D. M. H.; Orlemann, E. F. *J. Am. Chem. Soc.* **1949**, *71*, 2102.
(10) Cotton, S. *Lanthanides and Actinides*; Oxford University Press: New York, 1991.
(11) Loopstra, B. O. *Acta Crystallogr.* **1970**, *B26*, 656.
(12) Burns, P. C.; Finch, R. J. *Am. Mineral.* **1999**, *84*, 1456.
(13) Brown, D. *Halides of the Lanthanides and Actinides*; Wiley: London, 1968.
(14) Taylor, J. C. *Coord. Chem. Rev.* **1976**, *20*, 197.
(15) Penneman, R. A.; Ryan, R. R.; Rosenzweig, A. *Struct. Bonding* **1973**, *13*, 1.
(16) Halasyamani, P. S.; Willis, M. J.; Lundquist, P. M.; Stern, C. L.; Wong, G. K.; Poeppelmeier, K. R. *Inorg. Chem.* **1996**, *35*, 1367.
(17) Harrison, W. T. A.; Dussack, L. L.; Jacobson, A. J. *J. Solid State Chem.* **1996**, *125*, 234.
(18) Norquist, A. J.; Heier, K. R.; Stern, C. L.; Poeppelmeier, K. R. *Inorg. Chem.* **1998**, *37*, 6495.
(19) Francis, R. J.; Halasyamani, P. S.; Bee, J. S.; O'Hare, D. *J. Am. Chem. Soc.* **1999**, *121*, 1609.
(20) Halasyamani, P. S.; Walker, S. M.; O'Hare, D. *J. Am. Chem. Soc.* **1999**, *121*, 7415.
(21) Walker, S. M.; Halasyamani, P. S.; Allen, S.; O'Hare, D. *J. Am. Chem. Soc.* **1999**, *121*, 10513.
(22) Almond, P. M.; Deakin, L.; Porter, M. J.; Mar, A.; Albrecht-Schmitt, T. E. *Chem. Mater.* **2000**, *12*, 3208.
(23) Almond, P. M.; Talley, C. E.; Bean, A. C.; Peper, S. M.; Albrecht-Schmitt, T. E. *J. Solid State Chem.* **2000**, *154*, 635. (b) Talley, C. E.; Bean, A. C.; Albrecht-Schmitt, T. E. *Inorg. Chem.* **2000**, *39*, 5174.
(24) Francis, R. J.; Halasyamani, P. S.; O'Hare, D. *Chem. Mater.* **1998**, *10*, 3131.
(25) Francis, R. J.; Halasyamani, P. S.; O'Hare, D. *Angew. Chem., Int. Ed. Engl.* **1998**, *37*, 2214.
(26) Halasyamani, P. S.; Francis, R. J.; Walker, S. M.; O'Hare, D. *Inorg. Chem.* **1999**, *38*, 271.
(27) Francis, R. J.; Drewitt, M. J.; Halasyamani, P. S.; Ranganathachar, C.; O'Hare, D.; Clegg, W.; Teat, S. J. *Chem. Commun.* **1998**, 279.

10.1021/ic000921a CCC: $20.00
Published on Web 01/17/2001

and U(VI) products.[19,21,22,24,25] In contrast, the use of the aromatic amines as structure-directing agents in reactions of UO_3 with aqueous HF yields solely U(VI) products.[23] Use of these organic structure-directing agents has produced a wealth of new structure types with elaborate frameworks having no previously known counterparts.[19−27]

Herein we report the hydrothermal syntheses, structural characterization, and magnetic measurements of a new organically templated U(IV) aquofluoride, $[C_5H_{14}N_2][U_2F_{10}(H_2O)]$ (**AU2-3**). Although the magnetic behavior of compounds containing U(IV) ions has generally been interpreted on the basis of a $5f^2$ configuration, which has a $^3H_4$ ground state,[28,29] it is complicated by spin−orbit, crystal-field, and zero-field splitting effects on the temperature dependence of the susceptibility. Monomeric octacoordinated U(IV) complexes show effective moments ranging from 2.92 to 3.5 μ_B with Weiss constants θ ranging from −50 to −200 K, but with no long-range magnetic ordering.[30,31] Organically templated, low-dimensional uranium(IV) compounds, however, display evidence for antiferromagnetic[22,24,25] as well as metamagnetic-like transitions.[22]

Experimental Section

Synthesis. UO_3 (99.8%, Alfa-Aesar), HF (48 wt %, Aldrich), and homopiperazine (98%, Aldrich) were used as received. Distilled and Millipore filtered water was used in all reactions. The resistance of the water was 18.2 MΩ. *While the UO_3 contains depleted U, standard precautions for handling radioactive materials should be followed.* Elemental (CHN) microanalyses were performed by Atlantic Microlab, Inc. All reactions were run in Parr 4749 23 mL autoclaves with PTFE liners. The naming system for this compound stands for Auburn University, the dimensionality of the structure, and the compound number.[22]

UO_3 (572 mg, 2 mmol) and homopiperazine (301 mg, 3 mmol) were loaded in a 23 mL PTFE lined autoclave. Water (1 mL) was then added to the solids followed by the dropwise addition of HF (0.45 mL, 15 mmol). The autoclave was sealed and placed in a box furnace that had been preheated to 180 °C. After 72 h the furnace was cooled at 9 °C/h to 23 °C. The product consisted of a light-brown liquid over a mixture of green crystals of different colors and habits as follows: turquoise needles, $(C_5H_{14}N_2)_2U_2F_{12}\cdot 5H_2O$ (**AU1-2**);[32] deep-green truncated hexagonal bipyramids, $(C_2H_{10}N_2)U_2F_{10}$ (**AU2-1**);[22] green diamond-shaped plates, $(C_5H_{14}N_2)(UO_2F_{2.5})(UF_6)_{0.5}$ (**AU2-2**);[33] and pale-green rectangular plates, $[C_5H_{14}N_2][U_2F_{10}(H_2O)]$ (**AU2-3**). The mother liquor was decanted from the crystals, which were then washed with methanol and allowed to dry. **AU2-3** forms large loosely connected clusters of crystals that can be manually isolated from the other products with ease. Yield, 266 mg (34% yield based on U). Anal. Calcd for $C_5H_{16}N_2OF_{10}U_2$: C, 7.65; H, 1.93; N, 3.57. Found: C, 7.81; H, 2.08; N, 3.69.

Crystallographic Studies. Intensity data were collected from single crystals of **AU2-3** with the use of a Nicolet R3M single-crystal X-ray diffractometer. The data were processed, and an analytical absorption correction was applied. The structure was solved by direct methods and refined using the SHELXTL-93 package.[34] In these refinements, hydrogen atom positions were calculated with isotropic riding temperature factors. Disorder of the homopiperazinium dication through a mirror plane was straightforward to model; an apparent eight-membered ring results from the propyl and ethyl chains being superimposed. The nitrogen atoms in the homopiperazine ring were placed at sites where optimal hydrogen bonding was present. Some crystallographic details are listed in Table 1 for **AU2-3**. Additional crystallographic details are given in the Supporting Information.

Table 1. Crystallographic Data for $[C_5H_{14}N_2][U_2F_{10}(H_2O)]$ (**AU2-3**)

empirical formula	$C_5H_{16}N_2F_{10}OU_2$	formula mass	786.26
color, habit	pale-green, rectangular plate	space group	$P2_1/m$ (No. 11)
		temp (°C)	22
a (Å)	8.332(4)	λ (Å)	0.710 73
b (Å)	7.186(3)	ρ_{calcd} (g cm^{-3})	4.039
c (Å)	10.812(9)	μ(Mo Kα) (cm^{-1})	252.0
β (deg)	95.07(6)	$R(F)$ for $F_o^2 > 2\sigma(F_o^2)$[a]	0.0316
V (Å^3)	644.7(7)		
Z	2	$R_w(F_o^2)$[b]	0.0766

[a] $R(F) = \sum||F_o| - |F_c||/\sum|F_o|$. [b] $R_w(F_o^2) = [\sum[w(F_o^2 - F_c^2)^2]/\sum wF_o^4]^{1/2}$.

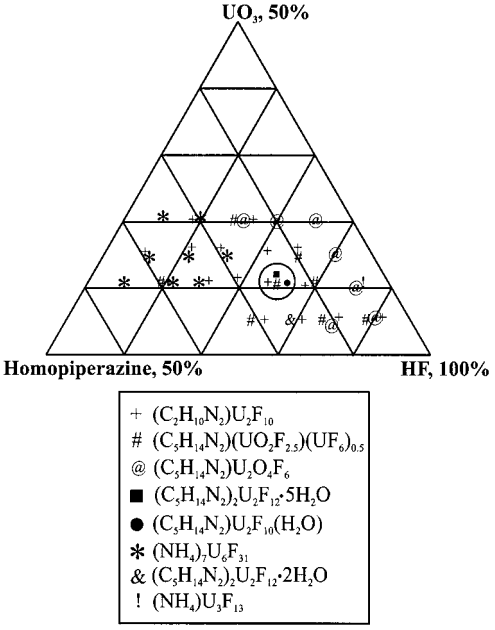

Figure 1. Compositional diagram for the UO_3/HF/homopiperazine system. Reactions were run in 1 mL of water at 180 °C for 72 h.

Magnetic Measurements. Magnetic data were measured on powders in gelcap sample holders with a Quantum Design PPMS 9T magnetometer/susceptometer between 2 and 300 K and in applied fields up to 9 T. Magnetic susceptibility measurements were made under zero-field-cooled conditions with an applied field of 0.5 T. Susceptibility values were corrected for the sample diamagnetic contribution according to Pascal's constants[35] (**AU2-3**: -278×10^{-6} emu/fu, fu ≡ formula unit) as well as for the sample holder diamagnetism.

Results and Discussion

Synthesis. The reaction of UO_3 with HF in aqueous media in the presence of homopiperazine for 72 h at 180 °C results in the formation of $(C_5H_{14}N_2)_2U_2F_{12}\cdot 5H_2O$ (**AU1-2**),[32] $(C_2H_{10}N_2)U_2F_{10}$ (**AU2-1**),[22] $(C_5H_{14}N_2)(UO_2F_{2.5})(UF_6)$ (**AU2-2**),[33] and $[C_5H_{14}N_2][U_2F_{10}(H_2O)]$ (**AU2-3**). All of these compounds except **AU2-3** can be prepared in pure form in other compositional regions as shown in Figure 1. In this series, we have focused

(28) Hutchison, C. A., Jr.; Candela, G. A. *J. Chem. Phys.* **1957**, *27*, 707.
(29) (a) Fournier, J.-M.; Tro, R. In *Handbook on the Physics and Chemistry of the Actinides*; Freeman, A. J., Lander, G. H., Eds.; Elsevier: New York, 1985 and references therein. (b) Martin, D. H. *Magnetism in Solids*; MIT Press: Cambridge, MA, 1967.
(30) Yoshimura, T.; Miyake, C.; Imoto, S. *Bull. Chem. Soc. Jpn.* **1974**, *47*, 515.
(31) Leask, M. J. M.; Osborne, D. W.; Wolf, W. P. *J. Chem. Phys.* **1961**, *34*, 2090.
(32) Almond, P. M.; Deakin, L.; Mar, A.; Albrecht-Schmitt, T. E. *J. Solid State Chem.*, manuscript in preparation.
(33) Almond, P. M.; Deakin,L.; Mar, A.; Albrecht-Schmitt, T. E. *Inorg. Chem.*, manuscript in preparation.
(34) Sheldrick, G. M. *SHELXTL PC, An Integrated System for Solving, Refining, and Displaying Crystal Structures from Diffraction Data*, version 5.0; Siemens Analytical X-Ray Instruments, Inc.: Madison, WI, 1994.
(35) Mulay, L. N.; Boudreaux, E. A. *Theory and Applications of Molecular Diamagnetism*; Wiley-Interscience: New York, 1976.

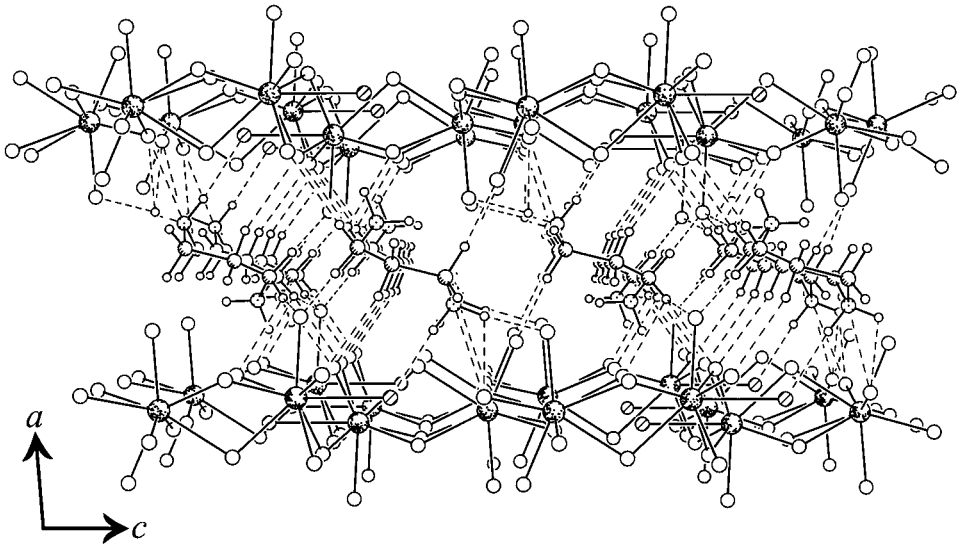

Figure 2. View along the *b* axis showing the layered structure of **AU2-3** with homopiperazinium dications separating the layers.

on compositions bordered by 50% UO_3, 50% homopiperazine, and 100% HF. At percentages near and above 50% UO_3, unreacted UO_3 predominates, whereas increased concentrations of homopiperazine will yield $(NH_4)_7U_6F_{31}$ and soluble uranium fluorides. **AU2-3** is unusual in that it can only be prepared at a single point in the compositional space diagram; variation in UO_3, HF, or homopiperazine content by as little as 5% precludes its formation. **AU1-2** also occurs initially at a single point in this diagram. However, crystals of **AU1-2** slowly grow from the mother liquors that yield $(NH_4)_7U_6F_{31}$.[32] All other compounds in the UO_3/HF/homopiperazine system have broad ranges of compositional stability. The correlation of pH of the solutions with the stability or dimensionality of the product remains unclear.

The reasons for the extraordinarily large number of compounds in the UO_3/HF/homopiperazine system are threefold. First, the seven-membered ring of homopiperazine is conformationally flexible and therefore can direct the formation of many different structures through hydrogen bonding. Homopiperazine was employed in these reactions for this reason because most other structure-directing amines do not have this property. Second, the concentration of homopiperazine in these reactions has a direct influence on the reduction of U(VI) to U(IV). As homopiperazine content is increased, U(IV) products predominate. Third, nucleophilic attack by fluoride on C−N bonds and oxidation by U(VI) give rise to both diprotonated ethylenediamine and ammonium cations, each of which will template the formation of different products. We speculate that the $[U_2F_{10}(H_2O)]^{2-}$ layers probably form through hydrolysis of the UO_3 to $[UO_2F_x]^{y-}$ species followed by reduction by excess homopiperazine to yield U(IV) units that subsequently polymerize into the extended structure observed. The reduction of U(VI) to U(IV) by homopiperazine is supported by other studies in the $UO_2(C_2H_3O_2)_2$/HF/pyridine and UO_3/HF/pyrazole systems, which have shown that the use of oxidation-resistant aromatic amines as structure-directing agents gives only U(VI) products.[23]

Structure. The structure of **AU2-3** is composed of $[U_2F_{10}(H_2O)]^{2-}$ sheets separated by homopiperazinium dications that form a strong hydrogen-bonding network between layers as illustrated in Figure 2. There are two crystallographically unique uranium centers, both of which have tricapped trigonal prismatic geometries. The environment around U(1) is formed from eight fluoride ligands and one water molecule, yielding $UF_8(H_2O)$ units. In contrast, U(2) is coordinated solely by fluoride ligands,

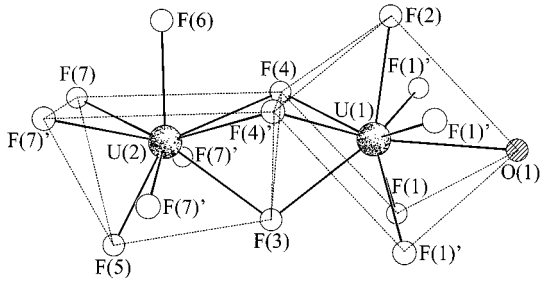

Figure 3. Face-sharing dimers built from $UF_8(H_2O)$ and UF_9 tricapped trigonal prisms in **AU2-3**.

producing UF_9 building blocks. U(2) shares one of its triangular faces from the trigonal prism with U(1) to form a dimeric unit (Figure 3). However, the shared triangular face of U(1) results from one of the capping ligands, not a face of the trigonal prism. The $UF_8(H_2O)$ and UF_9 polyhedra form $^1_\infty[UF_4F_{4/2}(H_2O)]$ and $^1_\infty[UF_5F_{4/2}]$ chains extending along the *b* direction through the sharing of two edges with units of the same type; i.e., each chain contains only $UF_8(H_2O)$ or UF_9. U(1)−U(1)′, U(2)−U(2)′, and U(1)−U(2) distances were found to be 3.995(2), 4.039(2), and 3.763(3) Å, respectively. These chains are then cross-linked together to form the two-dimensional sheets $^2_\infty[U_2F_{10}(H_2O)]^{2-}$ lying parallel to (100), as shown in Figure 4. The water molecules reside in 4.6 Å × 7 Å puckered, star-shaped channels that run down the *a* axis. When van der Waals radii are taken into account, the water molecules essentially fill these channels. The structure of these layers is in striking contrast to all other two-dimensional organically templated uranium compounds, which have only been reported to contain corner- and edge-sharing polyhedra.[19,22,24,25]

Selected bond distances for **AU2-3** are given in Table 2. U−F terminal and bridging distances range from 2.152(9) to 2.214(8) Å and from 2.278(6) to 2.528(6) Å, respectively. The U−O distance for the coordinated water molecule is 2.58(1) Å. This indicates that the longest bridging U−F distance is only 0.05 Å shorter than the U−O(H_2O) distance, leading to some ambiguity in assignment of F(4) as fluoride instead of oxygen, which is difficult to distinguish by X-rays alone. However, the substitution of oxygen for fluoride in the coordination sphere requires a formal oxidation state of +3 for U(1), which is unlikely because U(III) is readily oxidized to U(IV) without the exclusion of O_2. F(4) is asymmetrically bridging U(1) and

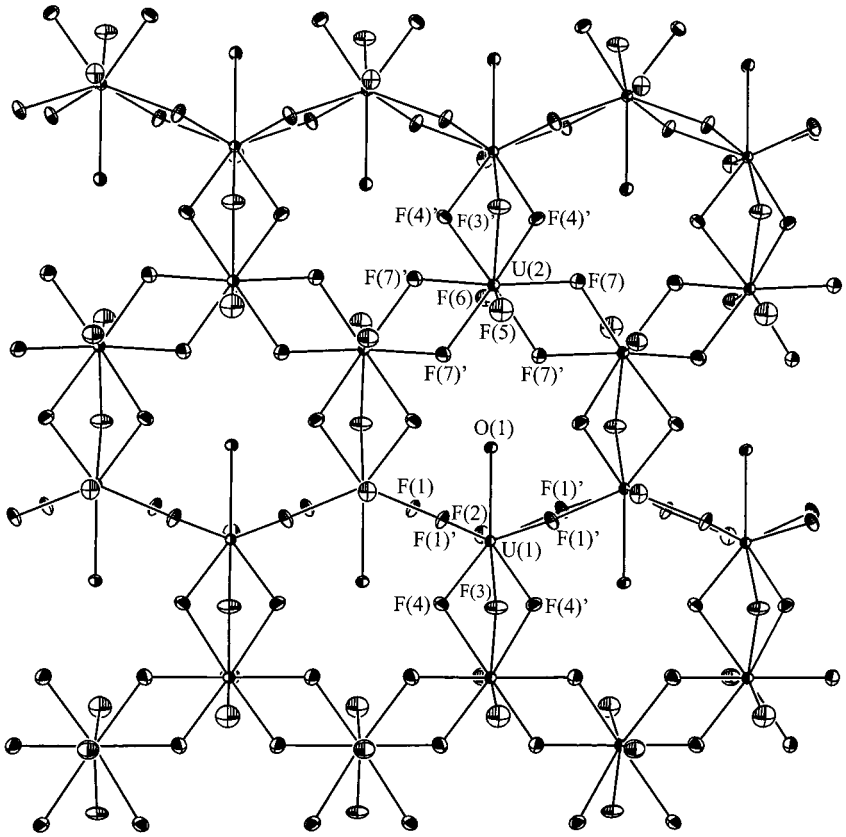

Figure 4. $[U_2F_{10}(H_2O)]^{2-}$ layer in **AU2-3** depicting the 4.6 Å × 7 Å puckered, star-shaped channels that run down the *a* axis where the coordinated water molecules reside. Atoms are shown as 50% displacement ellipsoids.

Table 2. Selected Bond Distances (Å) for $[C_5H_{14}N_2][U_2F_{10}(H_2O)]$ (**AU2-3**)

U(1)−F(1) (×2)	2.304(6)	U(2)−F(3)	2.378(9)
U(1)−F(1)′ (×2)	2.392(6)	U(2)−F(4) (×2)	2.528(6)
U(1)−F(2)	2.214(8)	U(2)−F(5)	2.152(9)
U(1)−F(3)	2.374(8)	U(2)−F(6)	2.182(9)
U(1)−F(4) (×2)	2.278(6)	U(2)−F(7) (×2)	2.348(7)
U(1)−O(1)	2.58(1)	U(2)−F(7) (×2)	2.386(6)
U(1)−U(1)′	3.995(2)	U(2)−U(2)′	4.039(2)
U(1)−U(2)	3.763(3)		

Table 3. Bond Valence Sums[37] for Atoms in $[C_5H_{14}N_2][U_2F_{10}(H_2O)]$ (**AU2-3**)

atom	*V*	atom	*V*
U(1)	4.05	F(4)	0.78
U(2)	3.95	F(5)	0.73
F(1)	0.86	F(6)	0.77
F(2)	0.82	F(7)	0.81
F(3)	0.79	O(1)	2.34

U(2) with U(1)−F(4) distances of 2.278(6) Å and U(2)−F(4) distances of 2.528(6) Å. The former distance is too short for this ligand to be water. Instead, this disparity can be explained by viewing the U(1)−F(4) distance as almost terminal and a secondary, long interaction that forms with U(2). The bond valence sums[36,37] for U(1) and U(2) are 4.05 and 3.95, respectively, which are consistent with the structure and formula assignments. Bond valences sums for the inorganic portion of **AU2-3** are listed in Table 3.

Magnetic Properties. A fit of the magnetic susceptibility of **AU2-3** above 150 K results in a paramagnetic Curie−Weiss temperature of $\theta = -15$ K. The effective moment μ_{eff}(300 K) of 5.20 μ_B/fu, which corresponds to 3.68 μ_B/U(IV), is larger than those observed in the $[U_2F_{10}]^{2-}$-layered compounds (3.23 μ_B/U(IV) in **AU2-1**[22] and 3.53−4.00 μ_B/U(IV) in **UFO-1** to **UFO-3**[24,25]) or in the $[U_2F_{12}]^{4-}$ chain compound **AU1-1** (3.09 μ_B/U(IV)).[22] As the temperature is decreased, the trend of decreasing effective moment, which noticeably drops below ∼50 K, is consistent with the presence of antiferromagnetic interactions between the U ions as well as the presence of the nonmagnetic singlet ground state of U(IV) (Figure 5).[38] The isothermal magnetization at $T = 2$ K (inset of Figure 5) exhibits a slight deviation from linearity at high fields ($M_{9T} = 1.26$ μ_B/

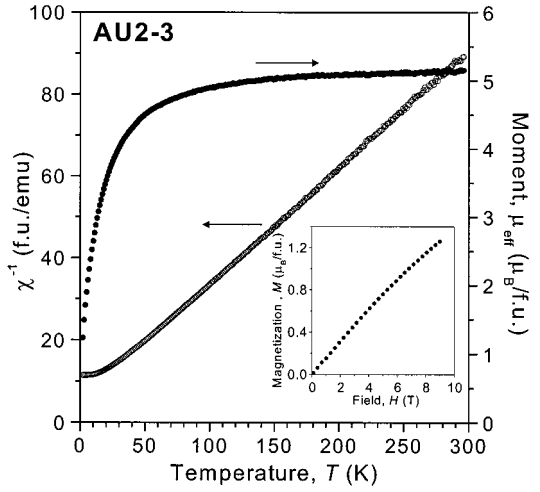

Figure 5. Effective moment and inverse magnetic susceptibility of **AU2-3** in an applied field of 0.5 T. Inset: Isothermal magnetization at $T = 2$ K.

(36) Brown, I. D.; Altermatt, D. *Acta Crystallogr.* **1985**, *B41*, 244.
(37) Brese, N. E.; O'Keeffe, M. *Acta Crystallogr.* **1991**, *B47*, 192.
(38) Santini, P.; Lémanski, R.; Erdös, P. *Adv. Phys.* **1999**, *48*, 537.

fu). The low-temperature magnetic behavior does not display evidence of long-range magnetic ordering but supports the formation of a nonmagnetic state as the magnetic susceptibility tends toward a temperature-independent value of 0.088 emu/fu below ~8 K.

Acknowledgment. This work was supported by NASA (Alabama Space Grant Consortium), NASA-EPSCoR, and Auburn University. Financial support from NSERC (Canada) and the University of Alberta is gratefully acknowledged.

Supporting Information Available: X-ray crystallographic file for **AU2-3** in CIF format. This material is available free of charge via the Internet at http://pubs.acs.org.

IC000921A